Biomaterials Science

ROYAL SOCIETY OF CHEMISTRY

PAPER

View Article Online
View Journal | View Issue

Cite this: *Biomater. Sci.*, 2024, **12**, 4483

Development of injectable colloidal solution forming an *in situ* hydrogel for tumor ablation†

Seong Jin Choi,[a,b] Sanghee Lee,[a] Hyunjun Choi,[a] Min Jun Ko,[a] Donghwan Kim *[b] and Dong-Hyun Kim *[a,c,d,e]

Received 29th April 2024,
Accepted 18th July 2024

DOI: 10.1039/d4bm00598h

rsc.li/biomaterials-science

Ablation cancer therapy using percutaneous intra-tumoral injection of ethanol is a promising method for targeted and effective locoregional cancer therapy. Magnetic gelatin microsphere (MGM) colloidal ethanol solution is developed as a potential injectable tumor ablation agent. The MGM was fabricated by electrostatic interactions among gelatin, acrylic acid, and acrylic acid-coated iron oxide nanoparticles. The fabricated MGM was dispersed in ethanol solution to form injectable MGM colloidal ethanol solution. The MGM colloidal ethanol solution can be easily infused and undergo *in situ* gelation *via* solvent exchange from ethanol to water in an artificial tissue. Furthermore, the MGM colloidal ethanol solution allowed doxorubicin (Dox) chemo-agent loading and its sustained release upon the formation of a drug depot by *in situ* gelation in artificial tissues. Our *in vitro* study demonstrated that locally delivered ethanol and Dox with MGM colloidal ethanol solution promoted the anti-cancer therapeutic efficacy with a significantly suppressed cancer cell recovery rate. Overall, our developed injectable MGM colloidal ethanol solution that can be transformed to a hydrogel drug depot at the injection site holds clinical potential for a new class of chemo-ablation agents.

Introduction

Ablation cancer therapy is increasingly being used as a treatment option, especially for patients who may not be suitable candidates for surgery or other traditional forms of treatment.[1,2] Ablation hydrogels are an emerging technology in the field of tumor treatment. These hydrogels are designed to deliver therapeutic agents directly to tumor sites while also providing a platform for localized ablation therapy.[3–5] Ablation therapy involves the destruction of tumor tissue using various methods such as the use of heat,[6] cold,[7] acid,[8] ethanol[9] and so on. Ablation gels can incorporate those elements that facilitate localized ablation. Intra-tumoral injectable ablation gels allow for precise targeting of tumor tissues, minimizing damage to the surrounding healthy tissue.[3,10] Injectable ablation gels offer potential for combination therapy approaches, where multiple treatment modalities such as chemotherapy,[11] immunotherapy,[12] and ablation therapy[13] can be integrated into a single platform for more effective tumor treatment. However, their continuously crosslinked volumes often exhibit large external dimensions and viscous rheological properties.[14] These properties lead to the backflow of the injected gels, uneven dispersion, and undesired release of the combined therapeutics during the applications.[15] Development of a new type of injectable ablation gel could have high impact on the treatment of various solid tumors.

Ethanol has been utilized for minimally invasive cancer ablation therapy and its conditions are well-established in interventional clinic fields.[9,16,17] However, the chemical properties of ethanol, such as low molecular weight, polarity, hydrophilicity, volatility, and rapid penetration, cause incomplete cell destruction and even cancer recurrence.[18] Combinational chemotherapeutics or immuno-therapeutics are essential for the desirable therapeutic outcome.[19,20] Herein, we developed injectable tumor ablation magnetic gelatin microsphere (MGM) colloidal ethanol solution that can be transformed to a hydrogel drug depot in the tissues. The MGM was fabricated with gelatin crosslinked with acrylic acid (AA) and AA-coated iron oxide nanoparticles (AA-IONP) *via* the water-in-oil emulsion method. Then the injectable MGM colloidal ethanol solution was formulated by dispersing MGMs in tumor ablative ethanol solution (Fig. 1a). An optimized size of

[a]*Department of Radiology, Feinberg School of Medicine, Northwestern University, Chicago, IL 60611, USA. E-mail: dhkim1@skku.edu, dhkim@northwestern.edu*
[b]*School of Chemical Engineering, Sungkyunkwan University (SKKU), Suwon 16419, Korea*
[c]*Robert H. Lurie Comprehensive Cancer Center, Northwestern University, Chicago, IL 60611, USA*
[d]*Department of Biomedical Engineering, McCormick School of Engineering, Northwestern University, Evanston, IL 60208, USA*
[e]*Department of Biomedical Engineering, University of Illinois, Chicago, IL 60607, USA*

† Electronic supplementary information (ESI) available. See DOI: https://doi.org/10.1039/d4bm00598h

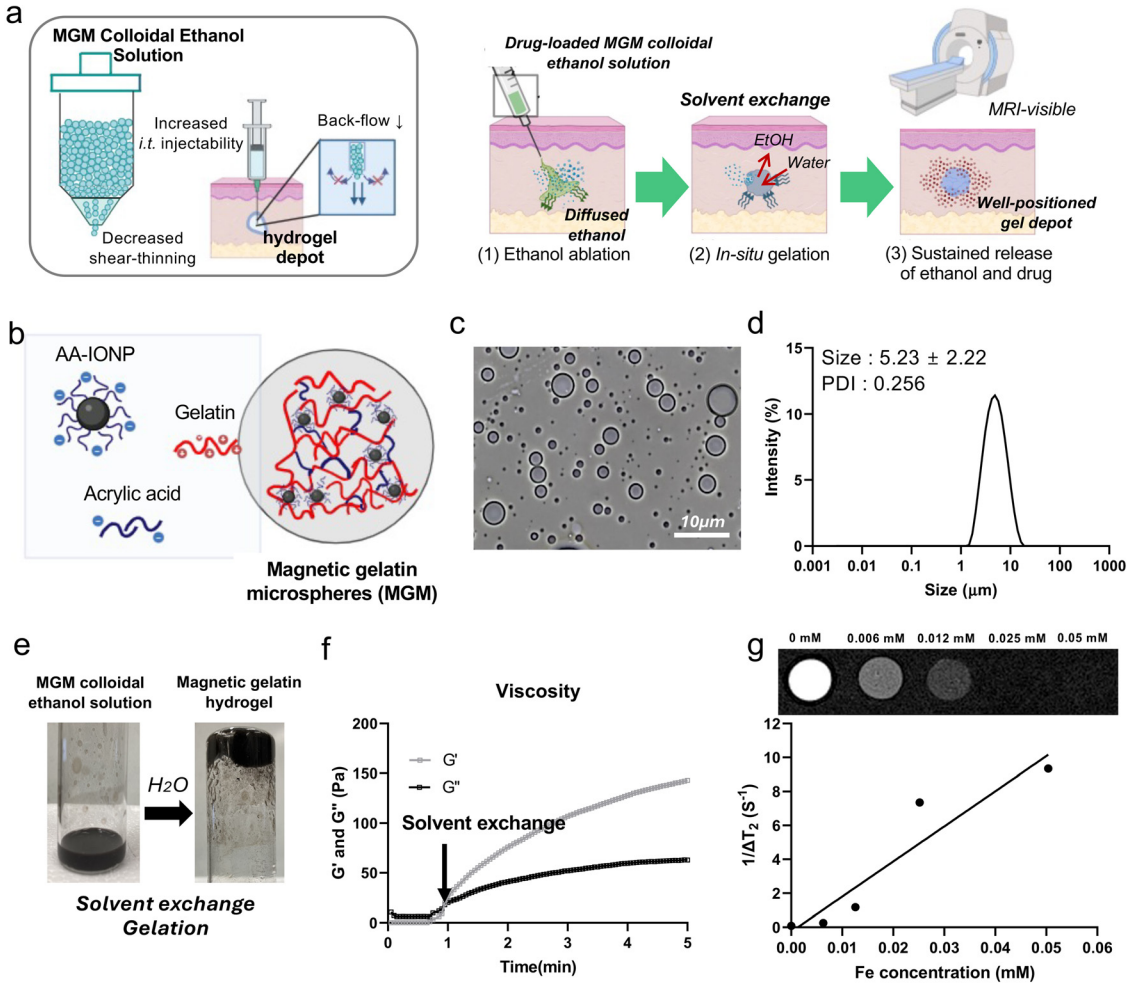

Fig. 1 (a) Schematic illustration of the injectable MGM colloidal ethanol solution with high injectability minimizing backflow and *in situ* gelation. (1) Injected MGM colloidal ethanol solution ablates tumors with ethanol. (2) The MGM is hydrated by the solvent exchange in an aqueous environment and (3) *in situ* gel formation at the injection site. The addition of magnetic nanoparticles and chemotherapeutic agents in the injectable MGM colloidal solution will allow MRI visibility and chemo-ablation cancer therapy. (b) Fabrication of MGMs using a gelatin matrix, acrylic acid, and AA-IONP in the emulsion method. (c) Optical microscopy image of fabricated MGMs. Scale bar is 10 μm. (d) Hydrodynamic size distribution of the MGM (n = 4). (e) Formulated injectable MGM colloidal ethanol solution and its *in situ* gelation through water introduction after 5 min. (f) Analysis of storage G' and loss G'' moduli during the MGM gel formation using a rheometer. Viscosity was measured for 5 min and water was introduced at 1 min. (g) T_2-Weighted MR images and concentration dependent T_2 relaxation of MGM colloidal ethanol solution in agarose phantoms (0, 0.125, 0.25, 0.5, and 1 mg mL^{-1} in 1% agarose).

MGMs in the colloidal solution allowed a stable injection without a significant backflow in an artificial tissue phantom. The injected colloidal solution was successfully converted to a hydrogel through the hydration of the MGM in the artificial tissue. Also, the well-positioned hydrogel depot from the injected MGM colloidal ethanol solution was capable of MRI monitoring during the procedure. Upon administration into the artificial tissues, the ethanol solution is exchanged with aqueous solution, causing the injected MGM to transform into a hydrogel. This novel behavior of the MGM colloidal ethanol solution will provide an additional option for the chemotherapeutic delivery during the ethanol ablation therapy. Here, a representative chemo-agent, doxorubicin (Dox), was loaded into MGMs, and their drug release kinetics and enhanced anti-cancer effect were investigated for combinational ethanol and Dox tumor ablation therapy. Our study highlights the potential of an injectable MGM colloidal ethanol solution ablation agent and provides optimized conditions to control injectability and physical properties. The developed ablation colloidal solution represents a promising avenue for the development of targeted and minimally invasive tumor ablation strategies, with the potential to improve outcomes and reduce side effects for patients with various types of cancer.

Results and discussion

Preparation of MGM colloidal ethanol solution and *in situ* gelation

Gelatin has high viscosity and gel-forming properties in an aqueous solution, which enable easy application and high

stability.[21] Also, IONP has been used as an MRI contrast agent for clinical applications.[22] Thus, these two substances are deemed suitable for MRI-visible injectable colloidal ethanol solution. AA-IONP were synthesized following our previous optimized protocol[23,24] and exhibited a nanoscale size (102 nm) and negative charge (−21 ± 2 mV) (ESI Fig. 1†). Electrostatic binding of the positive amine groups of gelatin and negative carboxyl groups of free AA and AA-IONP formed microspheres in the water-in-oil emulsion (Fig. 1b). 2 mg of AA was effectively counter-reacted with positively charged gelatin (100 mg) to generate gelatin microspheres (ESI Fig. 2†). The formed gelatin microspheres with 2 mg AA (3.8 mV) converted to negatively charged ones (−4.2 mV) by the addition of negatively charged AA-IONP (125 μg mL^{-1}). The fabricated MGM was 5 ± 2.22 μm in size as determined by microscopy and dynamic light scattering (DLS) (Fig. 1c and d). The MGM colloidal ethanol solution was formulated by the dispersion of the fabricated MGM in the ethanol solution (99%). The prepared MGM colloidal ethanol solution demonstrated *in situ* gel formation as the solvent was exchanged from ethanol to water (Fig. 1e). When the vial containing the MGM colloidal ethanol solution was added to the water and inverted, the transformed hydrogels did not flow down. *In situ* gelation of the MGM colloidal ethanol solution was also demonstrated in the measurement of viscosity. Within 1 minute after water addition, the G' and G'' values of the sample reached around 149.1 and 50.12 Pa, respectively (Fig. 1f). The IONP-embedded magnetic gelatin hydrogel was confirmed with the magnetic field responsiveness of the gel (ESI Fig. 3†). The formed hydrogel was also well visible in MRI T_2 images (Fig. 1g). The r_2 relaxivity of the gel was 206.97 mM^{-1} s^{-1} which can be used for MRI monitoring of gels during their ablative therapeutic applications.

Size control of MGM and syringe injectability of the MGM colloidal ethanol solution

Percutaneous intra-tumoral injection of ablation or therapeutic agents encounters some challenges in clinical trials, particularly regarding low injection efficiency based on dense tumor tissue characteristics.[25,26] Tumors typically exhibit higher interstitial fluid pressure due to complex vessel permeability, dense cell populations, and inadequate perfusion, making it difficult to penetrate with syringes or other delivery tools.[27,28] Furthermore, therapeutic agents delivered deep into the tumor tissue *via* syringes experience backflow movement, which complicates the determination of effective bioavailability in clinical uses.[29] Therefore, the injectability of therapeutic agents is a critical factor in the intra-tumoral delivery route for solid tumors.[30]

In the MGM colloidal ethanol solution, the size of the MGM is an important factor in the injectability, which affects how the MGM infiltrates the niche of tissues, well-dispersed, and covers the overall target tissues before the gelation. The size of the MGM can be controlled by changing the amount of AA-IONP at a fixed amount of gelatin and AA. Various amounts of AA-IONP from 1.9 to 500 μg mL^{-1} (Table 1) can be electrostatically encapsulated in the MGM, as demonstrated in the zeta-potential change (Fig. 2a). The addition of AA-IONP increased the negative charge up to −24 mV. However, excessive AA-IONP amounts over 125 mg did not further affect the zeta-potential change. 125 mg of AA-IONP could be the maximal capacity that can be effectively counter-reacted with gelatin (100 mg) and AA (6 mg) under the fabrication conditions. The size of the MGM in different amounts of AA-IONP was also dependent on the amount of AA-IONP. The addition of 1.95 μg mL^{-1} of AA-IONP could fabricate 4.1 μm of MGM. The size was decreased with an increased amount of AA-IONP. When 125 μg mL^{-1} of AA-IONP was added, the size of the MGM decreased to 0.93 μm. Excessive addition of AA-IONP over 125 μg mL^{-1} could not contribute to the size change of the MGM. This indicates that the increased amount of AA-IONP can lead to enhanced electrostatic interactions and result in smaller MGMs (Fig. 2b). The smallest size of fabricated MGMs (1 μm) under our experimental conditions showed an efficient syringe injectability of the MGM colloidal ethanol solution in various sized syringe needles. Comparative syringe injectability of samples was evaluated by measuring injection forces under each condition (Fig. 2c). The MGM colloidal ethanol solution including the smallest size of MGM (1 μm) showed a low syringe injection force less than 3 N regardless of the needle size (Fig. 2d). These forces were comparable with the syringe injection force (about 2 N) of the ethanol solution. However, conventional gelatin-gels have difficulty in passing through any type of needle and exhibit higher syringe injection forces over 10 N when the smallest diameter 20 G needle is used.

Table 1 AA-IONP amount dependent MGM samples at fixed amounts of gelatin (100 mg) and acrylic acid (6 mg) and their IONP loading efficiency

Sample	Gelatin (mg)	Acrylic acid (mg)	AA-IONP (μg mL^{-1})	IONP loading efficiency (%)
MGM1	100	6	500.00	35.70
MGM2			250.00	53.87
MGM3			125.00	99.82
MGM4			62.50	99.40
MGM5			31.25	99.49

Direct injection of MGM colloidal ethanol solution and *in situ* gelation in artificial tissue

To confirm that our developed MGM colloidal ethanol solution is appropriate for direct tissue injection, artificial tissues having similar mechanical properties to breast tissues using a 0.5% agarose phantom were prepared.[31] When the MGM-colloidal ethanol solution was injected into the agarose phantom tissue at a flow rate of 70 μl per minute, the whole volume of samples was injected without significant backflow and an *in situ* gel was formed (Fig. 3a). The injected MGM colloidal ethanol solution enabled the quick transformation from the MGM to magnetic hydrogel in the artificial tissue due to its hydration mediated gelation (ESI videos†). The

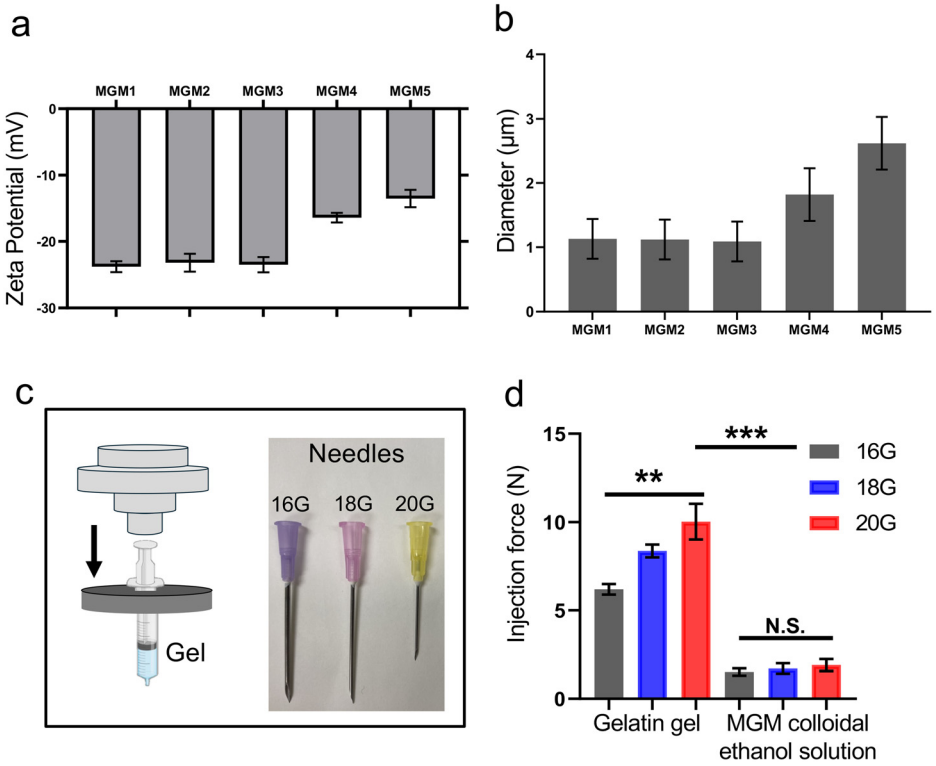

Fig. 2 (a) Zeta potential and (b) size changes of MGMs fabricated with various concentrations of AA-IONP (1.95–500 μg mL^{-1}) (each sample n = 5). (c) Experimental setup for measuring injection force and injection needles with different sizes (16 G, 18 G, and 20 G). (d) Measured injection force of the MGM colloidal ethanol solution and bulky gelatin-gels (n = 4) in different sizes of injection needles.

in situ formed gel was positioned like a spherical depot. However, the gelatin-gel (1 mg mL^{-1}) could not be infused inside the artificial tissue even at a slower or faster injection rate. The gelatin-gel demonstrated a backflow of around 80% of the injection volume, but the MGM-colloidal solution showed less than 7.7% backflow (Fig. 3b). These results are well consistent with a low syringe injection force of the MGM colloidal ethanol solution (Fig. 2d). The rapidly transformed MGM hydrogel within the tumor retains ethanol molecules, leading to enhanced ethanol ablation efficacy. Simultaneously, when additional anti-cancer agents are loaded into the MGM, these therapeutic agents remain within the hydrogel, providing sustained release at the injected tumoral site.

Additionally, the *in situ* formed hydrogel from the injected MGM colloidal ethanol solution was well visible in T_2 MRI. The MRI T_2 contrast effect of the hydrogel in the artificial tissue demonstrated a 7.3-fold higher contrast-to-noise ratio (CNR) compared to the non-contrasted gelatin gel (Fig. 3c and d). The high MRI contrast effect of the injected hydrogel is expected to be utilized for operative and post-operative imaging procedures. Furthermore, the *in situ* formed hydrogel from the MGM colloidal ethanol solution remained at the injection site of the artificial tissue over 7 days (Fig. 3e and f). Lower concentrations (0.1 and 0.25%) of agarose artificial phantom tissues corresponding to less dense tissues showed a faster diffusion of the formed hydrogel. In summary, the developed MRI visible MGM colloidal hydrogel demonstrated effective injectability in artificial tissues and MRI monitoring capability, and the structural integrity of the *in situ* hydrogel was maintained for a week. The MGM colloidal ethanol solution that delivers both the *in situ* formed hydrogel and ethanol can be used as a depot for the anti-cancer drug and ethanol in the tumor-tissue.

Anti-cancer drug loading into MGMs and enhanced cell killing effects of the MGM colloidal ethanol solution

MGMs can be used as a drug delivery carrier by loading various therapeutic agents during their fabrication. In chemo-ethanol ablation, ethanol increases the effectiveness of anti-cancer agents to damage tumor cells by enhancing the drug permeability.[32] Here, Dox, which can induce a synergistic anti-cancer effect with ethanol cancer cell ablation, was used as a model anti-cancer agent. Dox-loaded MGMs were formulated with different amounts of AA-IONP as shown in Table 2. A simple addition of Dox into the magnetic gelatin solution during the MGM fabrication efficiently loaded Dox into the MGM colloidal ethanol solution (Fig. 4a). The Dox loading efficiency was approximately 89% among all samples fabricated with the addition of 31–500 μg ml^{-1} AA-IONP in MGMs (Fig. 4b). The Dox release profile of the hydrogel from each MGM sample demonstrated AA-IONP amount dependent sustained Dox release over a week (Fig. 4c). Increased amount of AA-IONP, crosslinking MGM gel, decreased the Dox release rate.

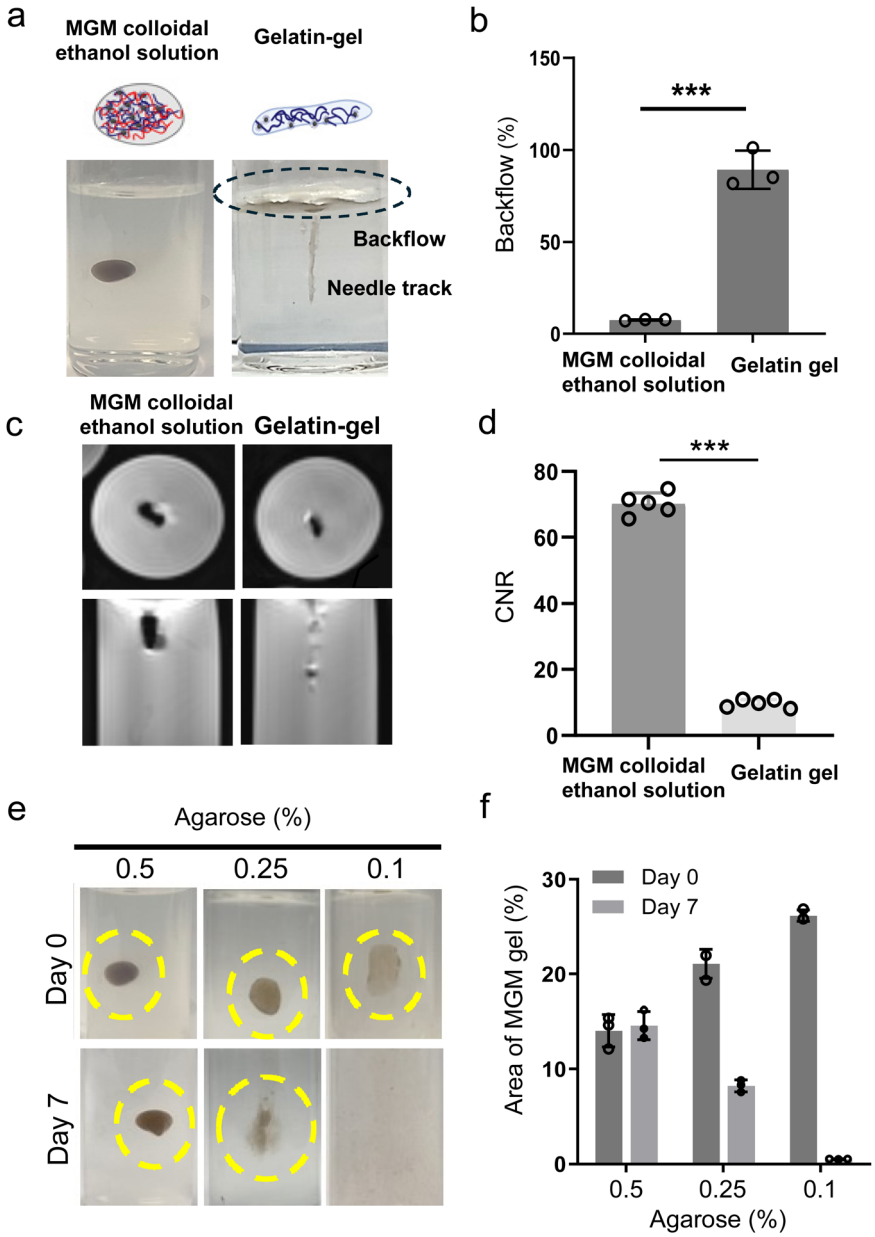

Fig. 3 (a) Images of the injected MGM colloidal ethanol solution and bulky gelatin-gel in a 0.5% agarose gel. (b) Measured backflow volume percentage in each injection of sample (MGM colloidal ethanol solution and gelatin-gel, n = 4). (c) MRI T_2 images of MGM colloidal ethanol solution and gelatin-gel. (d) CNR values of MGM colloidal ethanol solution and gelatin-gel (n = 5). (e) Images of infused MGMs at day 0 and day 7 in artificial tumor tissues, which are prepared with various agarose concentrations (0.1, 0.25 and 0.5%). (f) Time dependent distribution changes of MGM gels formed with the MGM colloidal ethanol solution in the phantom at 0 and 7-day post-infusion. The area of the color signal in each sample was measured with ImageJ (n = 3).

Finally, the anti-cancer cytotoxicity of the Dox-loaded MGM colloidal ethanol solution was assessed in two different cancer cell lines demonstrating long and short doubling times (Fig. 4d). Upon introducing the Dox-MGM colloidal ethanol solution into the upper chamber in a trans-well culture system, the solvent-exchange process within the cell culture medium solution led to *in situ* gelation, forming Dox-MGM-hydrogels. Then, the released ethanol and Dox rapidly permeated toward the tumor cell monolayer in the bottom chambers, inducing continuous cell death. Firstly, Dox-loaded MGM1 and Dox-loaded MGM5 were added to HeLa cancer cells (human cervical cancer, doubling time: 17.5 h). Although HeLa cells rapidly proliferate with the short doubling time, both MGM colloidal ethanol solution samples significantly induced cell death, with low viability (10.1% in MGM1 and 23.2% in MGM5) sustained for up to 3 days without the recovery of cell viability (Fig. 4e). As a control group, the cells were incubated with 20.0% ethanol (diluted final ethanol concentration of MGM colloidal

Table 2 Size, Dox loading efficiency, and loading contents of Dox-loaded MGM colloidal ethanol solution including MGM1 to MGM5

Sample	MGM diameter (μm)	Dox loading efficiency (%)	Dox loading contents (%)
MGM1 colloidal ethanol solution	3.42	88.14	2.36
MGM2 colloidal ethanol solution	2.81	87.75	2.35
MGM3 colloidal ethanol solution	2.62	87.78	2.35
MGM4 colloidal ethanol solution	1.82	88.64	2.38
MGM5 colloidal ethanol solution	1.09	90.64	2.43

ethanol solution). The ethanol-only treated group showed a recovery of cell viability over 3-day post-incubation. Ethanol treatment exhibited 37.9% cell viability one day post-incubation and the cell viability recovered up to 142% after only 3 days, representing a 4-fold increase in cell viability compared to that at day 1. Additionally, considering the sustained Dox release from the MGM hydrogel, a longer-term cytotoxicity test was performed using HepG2 cells (human liver cancer, doubling time: 44 h). After one day post-treatment, the cell viability was ~22.1% in both Dox-loaded MGM1 (fast Dox release) and MGM5 (slow Dox release) with mainly an ethanol cell killing effect (Fig. 4f). The low cell viability persisted until day 6 in cells incubated with Dox-loaded MGM5, whereas those of Dox-loaded MGM1 exhibited a growth recovery, reaching 47.1% viability at 6 days post-incubation. Ethanol-only treatment groups showed a rapid recovery of cancer cell viability. The results observed in HeLa cells incubated with ethanol only, the control group in HepG2 cells showed 35.4% cell viability one-day post-incubation and the recovery of cancer cell proliferation was exhibited with 142% cell viability in 6 days post-treatment.

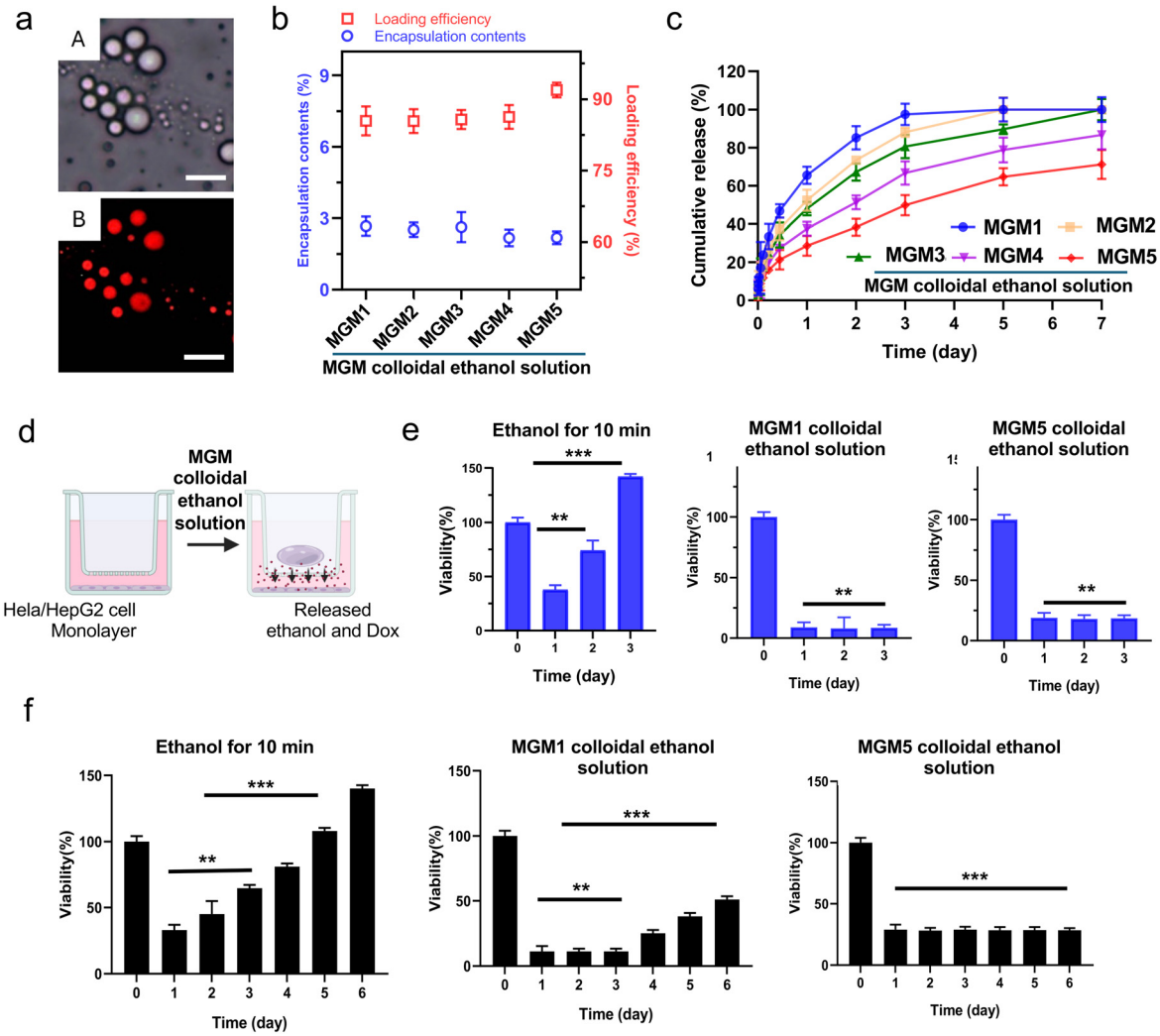

Fig. 4 (a) Optical microscopy image (top) and fluorescence images (bottom) of the Dox-loaded MGM colloidal ethanol solution. Scale bar is 10 μm. (b) Loading contents (blue at left *y*-axis) and loading efficiency (red at right *y*-axis) of the Dox-loaded MGM colloidal ethanol solution. (c) Drug release profiles of Dox-MGM-hydrogels (MGM1, MGM2, MGM3, MGM4, and MGM5) for 7 days. (d) *In vitro* trans-well experimental setup to confirm long-term cytotoxicity of the Dox-MGM colloidal ethanol solution. (e) Cell viability of HeLa cells followed up at day 3 (n = 5). (f) Cell viability of HepG2 cells followed up at day 7 (n = 5).

Ethanol ablation employs percutaneous infusion of ethanol into malignant tissue to induce necrosis through protein denaturation and cytoplasmic dehydration. Due to the simple, safe, and inexpensive procedures of the ethanol ablation technique with a low complication rate, ethanol ablation has been applied in the treatment of various solid tumors. However, the necessity of high-dose multiple treatment sessions, injection of large fluid volumes, and decreased efficacy with frequent recurrence in the treatment of non-capsulated tumors limit its applicability. The 5-year recurrence rate of ethanol ablation of hepatocellular carcinoma showed a 53.5% recurrence rate.[33] A combination of ablation and chemotherapy, known as chemo-ablation, is frequently considered as an effective cancer therapy in the clinic. Our developed MGM colloidal ethanol solution that can perform the combination chemoablation therapy in a single platform will provide an efficient way to enhance the therapeutic efficacy compared to each monotherapy or a simple additive combination chemo-ablation therapy. Future *in vivo* studies validating the efficacy of MGM colloidal ethanol solutions incorporating chemo- or immune modulating-agents with ethanol for the treatment of specific types of solid tumors are warranted. This research is crucial for potential translation into clinical applications.

Conclusions

Percutaneous intra-tumoral injectable tumor ablation colloidal solution that can be transformed to a hydrogel drug depot in the tissues was developed in this study. The MGM colloidal ethanol solution enhanced its syringe injectability compared to conventional injectable gels. The introduction of aqueous solvent to the colloidal ethanol solution showed *in situ* gelation. Our artificial tissue phantom study demonstrated that direct injection of the MGM colloidal ethanol solution minimized the backflow and generated a sustaining hydrogel depot at the injection site. Additionally, both MGM colloidal ethanol solution and MGM colloidal hydrogels demonstrated T_2 MRI contrast for monitoring the injected sample. Injectable MGM colloidal ethanol solutions can be used for intra-tumoral injection. This procedure is typically performed with image guidance, using various medical imaging techniques including ultrasound, X-ray DSA, MRI, and CT imaging. These imaging methods help localize the tumors to determine the precise injection site. The retention and biodistribution of the infused gel within the tumor are critical for effective treatment of the targeted tumor. Imaging-visible injectable formulations provide information about the distribution of injected agents within the tumor. This tracking and monitoring enable real-time procedural modifications and the prediction of therapeutic outcomes. The Dox anti-cancer agent was also readily loaded into the MGM. Regulating the amount of AA-IONP in the formulation could control the Dox release rate. Dox-loaded MGM hydrogels formed from the MGM colloidal ethanol solution demonstrated sustained and effective cell death compared to ethanol-only treatment, suggesting their potential as an effective chemo-ablation agent. The developed MGM colloidal ethanol solution that can be transformed into a hydrogel drug depot has considerable promise for an effective platform of tumor ablation therapy. This integrative and universal platform is expected to be utilized for delivering various types of chemo-agents and immunotherapeutic agents, including cytotoxic/cytostatic anti-cancer agents, immune checkpoint inhibitors, immune adjuvants, and more. As a result, its potential broad impact extends to applications such as ablation, local chemotherapy, local immunotherapy, and their synergistic combinations, enhancing cancer therapeutic outcomes.

Materials and methods

Materials/chemicals

Gelatin from porcine skin (gel strength, ~175 g bloom, Type A), sodium acetate (>98.5%), iron(III) chloride hexahydrate ($FeCl_3{\cdot}6H_2O$, >97%), sodium acrylate (NaAc, 97%), ethylene glycol ($(CH_2OH)_2$, >99%), and acrylic acid ($CH_2{=}CHCOOH$, >99%) were purchased from Sigma-Aldrich (Burlington, USA) and used as received without further purification. Doxorubicin hydrochloride was purchased in powder form from LC Laboratories (Woburn, USA).

Preparation and characterization of the MGM colloidal ethanol solution

To synthesize AA-IONP, we followed our previous work.[23] Briefly, 2 mmol of Fe, 2 mmol of $FeCl_3{\cdot}6H_2O$, and 150 mmol of H_2O were used for solution A, while solution B consisted of 6 mmol of NaOAc, 0.5 mmol of NaAc, and 50 mL of ethylene glycol. After stirring for 10 min at room temperature, a mixture of solutions A and B was used in the heat-up method to formulate AA-IONP. To prepare the MGMs, gelatin, acrylic acid, and AA-IONP were used as starting materials, and the water-in-oil emulsion method was utilized to formulate the micro-size particles. 100 mg gelatin and 6 mg acrylic acid were dissolved in 20 mL DI water. After stirring for 5 min, AA-IONP were added, and the solution was heated up to 50 °C for 10 min in a water bath. With subsequent sonication for 30 s, the solution was added dropwise to 50 mL of corn oil with 0.1 wt % Tween 80. A homogenizer (VWR headquarters, benchtop homogenizer, USA) was utilized to stir the corn oil at 6000 rpm for 10 min. The mixture was then stirred in an ice-water bath for another 1 h. To obtain the MGMs, the solvent exchange method was performed using ethanol.

Characterization of the MGM and MGM colloidal ethanol solution

Optical microscopy images were obtained using a scanning electron microscope (Zeiss, Supra 40, Germany). The particle size and surface charge (zeta potential) of MGMs were analyzed by dynamic light scattering (Malvern Instruments Ltd, Zetasizer Nano, Germany). The loading efficiency and loading contents were determined from the ultraviolet-visible absorbance of the AA-IONP peak (λ = 200–300 nm). Briefly, AA-IONP

were pelleted by centrifugation (3000*g*, 5 min, room temperature), and the supernatant was analyzed using a multimode microplate reader (BioTek, Synergy H1, USA). The drug loading efficiency and loading contents were calculated using the following formula:

$$\text{Loading efficiency}\,(\%) = (\text{Loaded amount of Dox})/(\text{Feeding amount of Dox}) \times 100$$

$$\text{Loading contents}\,(\%) = (\text{Loaded amount of Dox})/(\text{Total amount of MGM colloids}) \times 100$$

Rheological characteristics of the MGM colloidal ethanol solution

The rheological properties of MGM colloids were evaluated using a rotational rheometer (Anton Paar, MCR 72/92, USA) with a flat rotating plate and 1000 μm of gap distance. The sol–gel process was performed using the oscillation time for sweep measurement with a frequency of 1 Hz and a strain of 0.5%. The storage modulus (G') and loss modulus (G'') of the MGMs were observed by changing the angular frequency. In addition, the results of time sweep (0–10 min, 1 Hz) and frequency sweep (1–100 rad s^{-1}, strain of 1%) were collected at 37 °C by multiple continuous strain and time scan cycles.

Characterization of MRI T_2 contrast

The 1% agarose/PBS gel was utilized as an imaging phantom to characterize the MR imaging contrast effect. Samples were prepared with concentrations of 0, 0.25, 0.5, and 1 mg mL^{-1} of MGMs, and the r_2 relaxivity was calculated using a Bruker 7.0 T Clin Scan high-field small animal MRI system (Bruker BioSpin, Germany). To estimate the transverse relaxation time for each sample, coronal images were obtained at 6 echo times (TE) ranging from 60 ms to 120 ms with a repetition time of 1 s. The Miele-LXIV software (DICOM viewer) was employed to measure the signal, and the signal-to-noise ratio (SNR) was calculated using the equation SNR = S/N (S: signal intensity of ROI, N: background signal (noise)).

Measurement of injection force for syringe injectability

The injection force was analyzed using a Mechanical Testing Machine (MTS Systems Corporation, MTS 7, USA), with 16 G, 18 G, and 20 G needles (BD Biosciences, USA) utilized for testing. The prepared 5 mL samples (gelatin gel, MGM colloids), stored at 4 °C for 2 h, were loaded into 10 mL syringes and extruded through 16 G, 18 G, and 20 G needles. After fixing vertically under the mechanical testing machine, the upper compression plate was applied with a maximum force of 100 N, and the injection force required for the extrusion of the gel in the syringe was recorded.

Dox-loaded MGM colloidal ethanol solution and release profiles

Dox-loaded MGMs were prepared using a water-in-oil emulsion method. Gelatin and acrylic acid were dissolved in 20 mL of ultrapure water. After the addition of AA-IONP and Dox (1 mg mL^{-1}, 1 mL), this solution was warmed to 50 °C for 10 min. Followed by sonication for 30 s, the solution was added dropwise to 50 mL of corn oil with 0.1 wt% Tween 80. After stirring at 6000 rpm for 10 min, the mixture was stirred in an ice-water bath for another 1 h. To obtain the Dox-loaded MGMs, the solvent exchange method was performed with ethanol. Optical microscopy images were obtained using a scanning electron microscope (Zeiss, Supra 40, Germany) for the identification of Dox-loaded MGMs. To evaluate the kinetics of Dox release, the HTS Fluoro Block 24-Multiwell Insert System (Life Science, USA) containing 0.5 mL of MGM colloids was placed in a 24-well plate system containing PBS at 37 °C. After collecting the supernatant at predetermined time points, UV absorbance was analyzed with an excitation wavelength of 484 nm and an emission wavelength of 580 nm in comparison with the standard curve.

Phantom study for the injectability and MRI property of the MGM colloidal ethanol solution

Agarose phantoms were prepared using dry agar powder. The appropriate amount of agar powder was mixed into 50 mL of PBS and stirred until the powder was homogeneously dissolved in suspension. This mixture was brought to a boil for about 5 min until the agar was soluble in the solution. Varying concentrations (0.1, 0.25, 0.5, 1.0, and 1.5%) of agarose gel were utilized for analyzing the injectability of MGM colloids and gelatin-gel, at flow rates of 70 μl per minute using a syringe pump (New Era Pump Systems Inc, NE-300, USA). Magnetic resonance imaging (MRI) was used to measure the distribution of the gel. Additionally, the volume of the backflow quantity of MGM colloids was measured after 10 s and compared to the initial volume of MGM colloids. The dispersed area for each agarose gel concentration was quantified using ImageJ software by measuring the individual width of each gel. The contrast-to-noise ratio (CNR) in the phantom was measured with the SNR. The equation is $CNR = SNR_x - SNR_y$, where SNR_x: SNR of the background and SNR_y: SNR of the phantom treated with the sample.

Evaluation of the anti-cancer effect of the Dox-loaded MGM colloidal ethanol solution

HeLa cervical cancer and HepG2 hepatocellular carcinoma cells were obtained from the American Type Culture Collection (ATCC). The cells were cultured in Dulbecco's modified Eagle's medium (DMEM) supplemented with 10% fetal bovine serum (Thermo Scientific, USA) and 1% penicillin/streptomycin (Thermo Scientific, MA, USA). The cells were maintained at 37 °C with 5% CO_2 in a humidified incubator. The cytotoxicity of Dox was evaluated using the CCK-8 assay on HeLa and $HepG_2$ cells. $HepG_2$ cells were seeded under the filter in HTS Fluoro Block 24-multiwell Insert System plates at a density of 5×10^4 cells per well and then incubated overnight at 37 °C. To analyze the cytotoxicity of the MGM colloids, 1 mL of MGM colloids was treated, and the medium was replaced with fresh medium after washing. Cytotoxicity was assessed using the

CCK-8 assay at several incubation time points, according to the manufacturer's instructions. Briefly, after adding CCK-8 solution (Dojindo Molecular Technologies, USA) to each well, the cells were further incubated in the cell incubator for 2 h, and then the absorbance at 450 nm of each well was measured to calculate the cell survival rate.

Statistical analysis

Analysis was performed using GraphPad Prism (GraphPad). *T*-test was used on data with more than two groups. *P* values <0.05 were considered significant. $*p < 0.05$, $**p < 0.01$, $***p < 0.001$, and $****p < 0.0001$, if not indicated: not significant.

Author contributions

The manuscript was written through the contribution of all authors. All authors have given approval to the final version of the manuscript.

Data availability

All data from this project are available from the corresponding author upon reasonable request.

Conflicts of interest

There are no conflicts to declare.

Acknowledgements

This work was supported by grants R01CA218659 and R01EB026207 from the National Cancer Institute and National Institute of Biomedical Imaging and Bioengineering. This paper was also supported by the Korean Institute for Advancement of Technology (KIAT) grant funded by the Korea Government (MOTIE) (P0017305, Human Resource Development Program for Industrial Innovation (Global)).

References

1 J. M. Llovet, T. De Baere, L. Kulik, P. K. Haber, T. F. Greten, T. Meyer and R. Lencioni, *Nat. Rev. Gastroenterol. Hepatol.*, 2021, **18**, 293–313.
2 L. Kulik and H. B. El-Serag, *Gastroenterology*, 2019, **156**, 477–491.
3 G. R. Shin, H. E. Kim, J. H. Kim, S. Choi and M. S. Kim, *Pharmaceutics*, 2021, **13**, 1953.
4 F. Kadivar and M. C. Soulen, *J. Vasc. Interv. Radiol.*, 2010, **21**, S251–S256.
5 S. Ghai, A. Finelli, K. Corr, R. Chan, S. Jokhu, X. Li, S. McCluskey, A. Konukhova, E. Hlasny and T. H. van der Kwast, *Radiology*, 2021, **298**, 695–703.
6 Y. Minami, T. Aoki, S. Hagiwara and M. Kudo, *Cancers*, 2023, **15**, 4763.
7 K. Kwak, B. Yu, R. J. Lewandowski and D.-H. Kim, *Theranostics*, 2022, **12**, 2175.
8 R. Zhang, L. Wang, X. Wang, Q. Jia, Z. Chen, Z. Yang, R. Ji, J. Tian and Z. Wang, *Adv. Healthcare Mater.*, 2020, **9**, 2000394.
9 I. D. Hay, R. A. Lee and J. W. Charboneau, *J. Clin. Endocrinol. Metab.*, 2022, **107**, e2636–e2637.
10 A. Som, J. G. Rosenboom, E. Wehrenberg-Klee, A. Chandler, G. Ndakwah, E. Chen, J. Suggs, J. Morimoto, J. Kim and A. R. Mustafa, *Adv. Healthcare Mater.*, 2024, **13**, 2301848.
11 L. Li, H. Zhang, H. Zhao, D. Shi, C. Zheng, Y. Zhao and X. Yang, *Chem. Eng. J.*, 2022, **450**, 138421.
12 M. Chen, Y. Tan, J. Hu, Y. Jiang, Z. Wang, Z. Liu and Q. Chen, *Small*, 2021, **17**, 2104773.
13 J. S. Ribeiro, A. Daghrery, N. Dubey, C. Li, L. Mei, J. C. Fenno, A. Schwendeman, Z. Aytac and M. C. Bottino, *Biomacromolecules*, 2020, **21**, 3945–3956.
14 G. Jalani, D. H. Rosenzweig, G. Makhoul, S. Abdalla, R. Cecere, F. Vetrone, L. Haglund and M. Cerruti, *Macromol. Biosci.*, 2015, **15**, 473–480.
15 K. Kotani, F. M. Ngako Kadji, Y. Mandai and Y. Hiraoka, *Drug Delivery*, 2024, **31**, 2329100.
16 R. K. Gelczer, J. W. Charboneau, S. Hussain and D. L. Brown, *J. Med. Ultrasound*, 1998, **17**, 531–533.
17 X. Ding, L. Wang, Q. Liu, S. Chen, R. Jiang, L. Yu, P. Zhang, J. Lin, Y. Sun and X. Sheng, *Heart Rhythm*, 2024, **21**, 274–281.
18 D. S. Dwyer and R. J. Bradley, *Cell. Mol. Life Sci.*, 2000, **57**, 265–275.
19 Y. Chen, M. Yu, M. Liu, Y. Sun, C. Ling, M. Yu, W. Zhang, W. Zhang and X. Peng, *Adv. Sci.*, 2024, 2309760.
20 B. Yu, K. Kwak, R. J. Lewandowski and D.-H. Kim, *J. Vasc. Interv. Radiol.*, 2024, **35**(7), 1033–1042.
21 D. R. Bagal-Kestwal, M. Pan and B. H. Chiang, *Bio monomers for green polymeric composite materials*, 2019, pp. 117–140.
22 Z. Shen, A. Wu and X. Chen, *Mol. Pharm.*, 2017, **14**, 1352–1364.
23 B. C. Park, M. J. Ko, Y. K. Kim, G. W. Kim, M. S. Kim, T. M. Koo, H. E. Fu and Y. K. Kim, *Nat. Commun.*, 2022, **13**, 1144.
24 D. H. Kim, J. Chen, R. A. Omary and A. C. Larson, *Theranostics*, 2015, **5**, 477–488.
25 A. Hosseinpour, M. Soltani and M. Souri, *Sci. Rep.*, 2024, **14**, 1452.
26 Z. J. Senders and R. C. Martin, *Cancers*, 2022, **14**, 1754.
27 E. K. Rofstad and B. S. Mathiesen, *Neoplasia*, 2014, **16**, 586–594.
28 S. J. Lunt, T. M. Kalliomaki, A. Brown, V. X. Yang, M. Milosevic and R. P. Hill, *BMC Cancer*, 2008, **8**, 1–14.
29 F. Casanova, P. R. Carney and M. Sarntinoranont, *PLoS One*, 2014, **9**, e94919.

30 N. M. Muñoz, M. Williams, K. Dixon, C. Dupuis, A. McWatters, R. Avritscher, S. Z. Manrique, K. McHugh, R. Murthy and A. Tam, *J. Immunotherap. Cancer*, 2021, **9**, e001800.
31 A. M. Teixeira and P. Martins, *J. Biomater. Appl.*, 2020, **34**, 1163–1170.
32 R. Gupta, Y. Badhe, B. Rai and S. Mitragotri, *RSC Adv.*, 2020, **10**, 12234–12248.
33 S. Shiina, R. Tateishi, M. Imamura, T. Teratani, Y. Koike, S. Sato, S. Obi, F. Kanai, N. Kato, H. Yoshida, M. Omata and K. Koike, *Liver Int.*, 2012, **32**, 1434–1442.